tvst

Retina

Inner Retinal Changes in Acute Experimental BRVO Treated With Bevacizumab or Triamcinolone Acetonide

Ian L. McAllister[1–3], Sarojini Vijayasekaran[1,2], Riyaz Bhikoo[2,3], Fred K. Chen[1–4], Dan Zhang[1,2], Emily Kanagalingam[1,2], Samuel McLenachan[1,2], and Dao-Yi Yu[1,2]

[1] Centre for Ophthalmology and Visual Science, The University of Western Australia, Perth, Australia
[2] Lions Eye Institute, The University of Western Australia, Perth, Australia
[3] Department of Ophthalmology, Royal Perth Hospital, Perth, Australia
[4] Ophthalmology, Department of Surgery, University of Melbourne, East Melbourne, Australia

Correspondence: Ian L. McAllister, Lions Eye Institute, The University of Western Australia, 2 Verdun Street, Nedlands, WA 6009, Australia.
e-mail: ian.mcallister@lei.org.au

Received: July 1, 2022
Accepted: January 9, 2023
Published: February 8, 2023

Keywords: branch retinal vein occlusion; neurodegeneration; apoptosis; bevacizumab; triamcinolone acetonide

Citation: McAllister IL, Vijayasekaran S, Bhikoo R, Chen FK, Zhang D, Kanagalingam E, McLenachan S, Yu DY. Inner retinal changes in acute experimental BRVO treated with bevacizumab or triamcinolone acetonide. Transl Vis Sci Technol. 2023;12(2):11, https://doi.org/10.1167/tvst.12.2.11

Purpose: Apoptosis is a key process in neural degeneration associated with retinal vascular diseases. Vascular endothelial growth factor (VEGF) antagonists, including bevacizumab, are used to treat macular edema in these diseases. As VEGF has a critical role in the preservation of retinal neuronal cells, this study investigates the effects of bevacizumab on neural damage in a pig model of branch retinal vein occlusion (BRVO) and compares it with triamcinolone acetonide (TA) which is reported to possess neuroprotective properties.

Methods: Thirty-six pigs had a photothrombotic BRVO in both eyes. Six pigs were injected with bevacizumab in one eye and TA in the fellow eye, then they were sacrificed, the eyes enucleated, and retinas processed at 2, 6, 10, and 20 days, respectively, together with three pigs (six eyes) BRVO only and three normal pigs (six eyes). Neuronal degeneration (apoptosis) and associated inner retinal changes were determined by terminal deoxyynuclotidyl transferase dUTP nick-end labeling (TUNEL), histology, and immunohistochemistry for macrophages.

Results: TUNEL labeling showed significantly higher apoptosis rates in the ganglion cell layer (GCL) and the inner nuclear layer (INL) in the bevacizumab-treated compared with the TA-treated retinas at 2, 10, and 20 day time points after occlusion ($P < 0.05$). Pyknotic cells were significantly higher in the GCL in bevacizumab-treated eyes at 6, 10, and 20 days and in the INL at 2 days compared to TA-treated retinas ($P < 0.05$). Macrophage infiltration was seen at all time points in both untreated and treated retinas with an absence of significance between bevacizumab- and TA-treated retinas ($P > 0.05$).

Conclusions: Neurodegeneration in the BRVO acute phase is exacerbated by current standard treatments for BRVO. These results may have implications for the timing and treatment type.

Translational Relevance: In the acute phase of BRVO, VEGF suppression with bevacizumab and to a lesser extent with triamcinolone exacerbates apoptosis in the inner retinal layers, which has implications for both the timing and choice of treatment.

Introduction

Retinal vein occlusion (RVO) is a spectrum of ischemic microvascular retinal disease that may affect either a branch vein (branch vein occlusion, BRVO) or the central retinal vein and remains a common cause of unilateral vision loss. In more than 90% of those affected by a RVO, a decrease in vision secondary to macular edema (ME), caused by the breakdown of the blood–retina barrier, and the efflux of fluid from permeable vessels occurs.[1] BRVO is the most common retinal vascular pathology after diabetic retinopathy, with an incidence of 2.14/1000 per year in those over

40 year of age.[2–4] Without treatment, it can lead to a sustained loss of vision, with a reported final mean visual acuity of 20/70, with 23% of patients having a visual acuity of ≤20/200.[5,6] RVOs contribute to 3.6% of bilateral visual reductions in those 65 years of age or older.[7] Few patients improve without treatment to better than 20/40 vision. The impact on patients with unilateral BRVO has been shown to have a detrimental effect on vision-related quality of life.[8]

Treatments that have improved the outcomes of BRVO over the natural history have included grid laser photocoagulation[6] and intravitreal steroids.[9] The advent of intravitreal vascular endothelial growth factor (VEGF) antagonists, however, has led to these agents becoming accepted first-line therapy for most patients with this condition. Intravitreal anti-VEGF therapy initially with ranibizumab in the BRAVO study[10] and aflibercept in the VIBRANT study[11] confirmed the effectiveness of these agents in achieving significantly better vision than other treatments. Neither, however, restored mean visual acuities to normal levels, and for some patients the treatment burden is significant with extended durations of therapy required. Anti-VEGF therapy is very effective in resolving ME by controlling permeability in the short term; however, they appear to be less effective in reversing the changes in the regulation of several inflammatory cytokines and factors or the cell death that plays a critical role in the pathogenesis of BRVO.

Programmed cell death (apoptosis) of neuroretinal cells, including Müller, amacrine, and ganglion cells (GCs), is considered to be the leading process resulting in the neural degeneration associated with these diseases.[12,13] It occurs early in the course of the occlusion, is progressive, and is currently irreversible. These cells are initially in a pre-apoptotic state undergoing pyknosis, and subsequent death can be very slow and variable, culminating in phagocytic uptake by macrophages as the disease progresses.[14]

We have previously demonstrated that apoptosis of neuronal cells occurs early in the acute (2–20 days) phase in BRVO in the pig model accompanied by inflammation and breakdown of osmohomeostasis reflected by changes in the levels of cytokines and factors.[15] Remarkably, VEGF upregulation was early, brief, and inconsistent in the acute phase in this study. VEGF has a critical role in the preservation of retinal neuronal and endothelial cells to maintain homeostasis, ensuring cell function and its survival.[16,17] This leads to the possibility that, before it is fully upregulated in the acute phase, as seen in our study, early suppression with VEGF antagonists, when neural elements are in a vulnerable phase, may paradoxically further exacerbate neuronal degeneration.

In order to determine the effect of early suppression of VEGF on retinal neuronal degeneration and the most beneficial timing of anti-VEGF treatment for successful amelioration of this progressive event, we have investigated the anti-VEGF agent bevacizumab in a pig model of BRVO. We also investigated the steroid triamcinolone acetonide (TA) to compare it with bevacizumab, as steroids have also been shown to inhibit overexpression of VEGF and are effective in resolving extracellular and intracellular edema and leakage while also providing neuroprotective, anti-apoptotic, and anti-inflammatory therapeutic effects.[18]

Materials and Methods

Animals

All animal procedures were approved by the Animal Ethics Committee of the University of Western Australia in accordance with the National Health and Medical Research Council's *Australian Code of Practice for the Care and Use of Animals for Scientific Purposes* (8th edition); they conformed to the ARVO Statement for the Use of Animals in Ophthalmic and Vision Research and the policies in the "Guide to the Care and Use of Laboratory Animals" issued by the National Institutes of Health. All efforts were made to minimize pain and suffering during surgery, and the animals were housed under great care at all times to provide an untroubled and comfortable environment.

Surgery and Tissue Processing

Ten-week-old female pigs (body weight, ~30 kg) were used in this study. The pigs were anesthetized and sedated with a combination of zolazepam and tiletamine (4 mg/kg Zoletil 100; Virbac Australia, Milperra, NSW, Australia) and xylazine (2 mg/kg Xylazine, 100 mg/mL Ilium Xylazil; Troy Laboratories, Glendenning, NSW, Australia) by intramuscular injection in the trapezius muscle of the neck. With the pig in sternal recumbence, a branch of the right auricular vein was cannulated, and propofol (1–2 mg/kg Vetofol 1%; Norbrook Laboratories, Tullamarine, VIC, Australia) was administered by intravenous injection to facilitate oral endotracheal intubation with a 6-, 6.5-, 7- or 7.5-mm internal diameter cuffed endotracheal tube (Portex; Smiths Medical, Plymouth, MN). General anesthesia was maintained with

isoflurane (1 mL/mL 0.5%–2% Attane Isoflurane; Bayer Australia, Pymble NSW, Australia) in oxygen delivered via a circle breathing system. The pigs breathed spontaneously during the procedure. Intraoperative monitoring included oxyhemoglobin saturation and pulse rate as measured with a pulse oximeter placed on the pinna and capnography (SurgiVet V9203 multivariable monitor; GCX Corporation, Petaluma, CA). These parameters were measured continuously and recorded every 5 minutes on a paper anesthetic record. The multimodal analgesia regime included analgesia from tiletamine and xylazine in addition to carprofen (4 mg/kg Carprieve 50 mg/mL; Norbrook, Newry, Northern Ireland) by subcutaneous injection or meloxicam (0.5 mg/kg Ilium Meloxicam 20; Troy Laboratories) by intramuscular injection after the induction of anesthesia. Pupillary dilation was achieved with tropicamide 1% and phenylephrine hydrochloride 2.5%.

Baseline assessment was performed in all eyes using binocular indirect ophthalmoscopy to exclude preexisting retinal disorders. An intravenous injection was administered via an ear vein of 10 mg/kg rose bengal dye (Sigma-Aldrich, St. Louis, MO), which is a dye with peak absorption of light close to the wavelength of the argon laser. This allows an intravascular thrombus to be created with minimal damage to the vessel wall if appropriate laser powers are used. A photothrombotic BRVO was created in an inferior vein adjacent to the optic disc in both eyes of each pig using a 532-nm wavelength laser (Ellex Medical Lasers, Adelaide, SA, Australia) as described previously.[15] This vein was chosen as it creates a small superior field defect and leaves the horizontal and inferior fields unaffected.

After laser photocoagulation and subsequent intravitreal injection, chloramphenicol ointment 1% (Sigma Healthcare, Rowville, VIC, Australia) was applied to the eyes, and the pigs were allowed to recover. At each endpoint, the pigs were euthanized with a two-step technique: zolazepam, tiletamine, and xylazine by intramuscular injection as above, followed by intravenous injection of pentobarbitone (160 mg/kg Lethabarb Euthanasia Injection 325 mg/mL; Virbac Australia).

Three pigs (six eyes) were sacrificed at each 2-, 6-, 10-, and 20-day time point after BRVO without treatment. Further groups of six pigs were injected with TA (Kenacort A40; Aspen Pharmacare Australia, St. Leonards, NSW, Australia) in one eye chosen randomly and with bevacizumab (Baxter Healthcare Australia, Old Toongabbie NSW, Australia) in the fellow eye immediately after BRVO creation; they were sacrificed at the same time points after surgery.

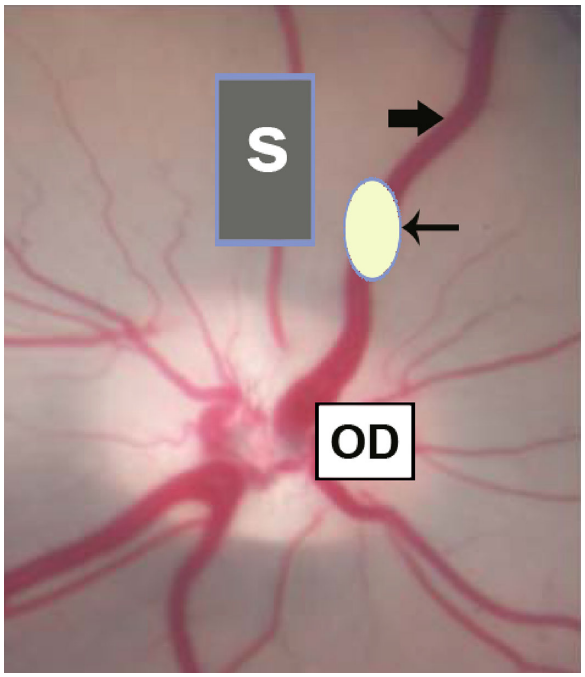

Figure 1. Schematic representation of regions for photocoagulation (*thin arrow*) and dissected sample (S) using a vein (*thick arrow*) superior to the optic disc (OD) as an orientation marker.

Three pigs (six eyes) were used as normal controls and sacrificed with no intervention. Immediately after sacrifice, the eyes were enucleated, and the anterior segment was removed. A piece containing the laser burn was excised. In addition, two pieces on either side of the laser burn within the area of the BRVO, inside 5 mm of the occluded vein and approximately 2 × 3 mm in dimension, were also dissected. In all eyes, the same region of the retina was sampled (Fig. 1). One piece was stored away for further cytokine studies. The other piece was again bisected; one piece was fixed in 4% paraformaldehyde overnight at 4°C and processed in paraffin for immunohistochemistry, terminal deoxyynuclotidyl transferase dUTP nick-end labeling (TUNEL), and basic histology. Paraffin processing was consistent for all samples on an automated tissue processing machine (TP1020; Leica, Wetzlar, Germany) with a set program (adapted from Ref. 19) for all processing. The other piece was fixed in 2.5% glutaraldehyde in 0.1-M phosphate buffer and processed in epoxy resin also on an automated processing machine (Lynx II Automated Tissue Processor; Electron Microscopy Sciences, Hatfield, PA) with presettings constant for all samples (adapted from Ref. 19) for transmission electron microscopy (TEM). Similar areas of the normal eyes without a BRVO were also dissected and similarly processed.

TUNEL Technique

Apoptosis was assessed by TUNEL, which labels fragmented DNA, an indicator of cell death, and pyknosis (early changes of nuclear shrinkage and chromatin condensation) was analyzed by histology and ultrastructure to assess architectural changes. Macrophage immunocytochemistry was performed, as macrophages are involved in the end stage in apoptosis and implicated in BRVO. Comparable regions of the retinas were used for the TUNEL, pyknosis, and immunohistochemistry analyses. Measures were taken to maintain consistency in all assays.

The TUNEL technique, which is widely employed to measure DNA fragmentation to highlight apoptotic cells in tissues, was used to detect cell death. The staining procedure was identical for all slides with respect to concentration of solutions and incubation times. Briefly, 6-µm sections were deparaffinized, permeabilized by subjection to heating in a microwave for 4 minutes in sodium citrate buffer (pH 6.0), and labeled according to manufacturer's protocol (In Situ Cell Death Detection Kit, Fluorescein; Roche Diagnostics, Penzberg, Germany). Sections were labeled by incubating them with a TUNEL reaction mixture consisting of 50 µL of enzyme solution (terminal deoxynucleotidyl transferase) and 450 µL of label solution (nucleotide mixture fluorescein–dUTP) in a humidified chamber at 37°C in the dark for 60 minutes. Positive and negative controls were incubated with DNase I recombinant (1500 U/mL in 50-mM Tris, pH 7.5; 10-mM $MgCl_2$; 1-mg/mL bovine serum albumin) for 10 minutes at room temperature to induce DNA strand breaks or with the enzyme incubation step omitted, respectively. Slides were rinsed in phosphate-buffered saline (PBS) containing a nuclear stain (Hoechst; Sigma-Aldrich) which stains the DNA of all cells,[20] mounted with antifade medium, stored at 20°C, and viewed the following day under an epifluorescent microscope equipped with a fluorescence-relevant detection filter (excitation/emission maxima, 330/560 nm). Photographs were taken at preset settings on the microscope that included sensitivity, light intensity, and the position of all other filters; the same settings were used for all sections at a magnification of 60× oil immersion. TUNEL-positive cells and all Hoechst-stained nuclei (total cells) were manually counted by two people. Hematoxylin and eosin (H&E)-stained pyknotic and non-pyknotic nuclei were also counted.

For cell death, pyknosis and immunocytochemistry of CD163 (a macrophage marker), one image each from four randomly selected sections were examined from each sample (eye) of each group (normal, untreated, bevacizumab, and TA-treated BRVO) at each time point from five eyes (20 images) each. In each image, TUNEL-positive cells and all Hoechst-stained nuclei (total cells) were manually counted by two people. Hematoxylin and eosin (H&E)-stained pyknotic and non-pyknotic nuclei were also counted.

For TUNEL, pyknosis (H&E staining), and macrophage immunohistochemistry, sections were obtained from five eyes from three pigs for the normal eye and untreated BRVO, and sections were obtained from five eyes from five pigs for the treated eyes (TA and bevacizumab), and images of the field of view at 60× magnification were captured.

For TUNEL, in normal eyes, total cells in four images counted at 2 days after BRVO included 63 to 142 in the ganglion cell layer (GCL) and 289 to 525 in the inner nuclear layer (INL). In the untreated eye at 2 days after BRVO, 79 to 174 were counted in the GCL and 299 to 544 were counted in the INL; at 6 days after BRVO, 76 to 189 were counted in the GCL and 216 to 426 were counted in the INL; at 10 days after BRVO, 116 to 145 were counted in the GCL and 218 to 382 were counted in the INL; and at 20 days after BRVO, 103 to 198 were counted in the GCL and 285 to 595 were counted in the INL.

In the TA-treated eyes, total cells in four images counted at 2 days after BRVO included 55 to 127 in the GCL and 473 to 711 in the INL; at 6 days after BRVO, 80 to 170 were counted in the GCL and 459 to 759 in the INL; at 10 days after BRVO, 51 to 79 were counted in the GCL and 488 to 662 in the INL; and at 20 days after BRVO, 55 to 116 were counted in the GCL and 323 to 688 in the INL.

In the bevacizumab-treated eyes, total cells in four images counted at 2 days after BRVO included 90 to 174 in the GCL and 419 to 970 in the INL; at 6 days after BRVO, 84 to 180 were counted in the GCL and 216 to 556 in the INL; at 10 days after BRVO, 56 to 116 were counted in the GCL and 149 to 700 in the INL; and at 20 days after BRVO, 35 to 213 were counted in the GCL and 167 to 670 in the INL.

For pyknosis in the normal eye, total cells in four images counted at 2 days after BRVO included 29 to 89 in the GCL and 227 to 446 in the INL. In the untreated eye 2 days after BRVO, 98 to 214 were counted in the GCL and 476 to 841 in the INL; at 6 days after BRVO, 78 to 266 were counted in the GCL and 292 to 707 in the INL; at 10 days after BRVO, 48 to 126 were counted in the GCL and 393 to 673 in the INL; and at 20 days after BRVO, 62 to 96 were counted in the GCL and 279 to 506 in the INL.

In the TA-treated eyes, total cells in four images counted at 2 days after BRVO included 65 to 223 in the GCL and 117 to 868 in the INL; at 6 days after BRVO, 53 to 143 were counted in the GCL and 380 to 718 in the INL; at 10 days after BRVO, 57 to 62 were counted in the GCL and 383 to 644 in the INL; and at 20 days

after BRVO, 55 to 131 were counted in the GCL and 317 to 649 in the INL.

In the bevacizumab-treated eyes, total cells in four images counted at 2 days after BRVO included 101 to 188 in the GCL and 614 to 639 in the INL; at 6 days after BRVO, 87 to 345 were counted in the GCL and 254 to 690 in the INL; at 10 days after BRVO, 72 to 165 were counted in the GCL and 152 to 656 in the INL; and at 20 days after BRVO, 67 to 118 were counted in the GCL and 184 to 689 in the INL.

For the immunohistochemistry of macrophages, primary counts of macrophages were obtained from the field of view of the retina (200 µm length) of four images from normal eyes and from each group at each time point (20 images).

Histology

Basic histological analysis was performed on H&E-stained 6-µm paraffin sections and viewed by light microscopy (LM; Eclipse E800; Nikon, Tokyo, Japan). Martius Yellow Scarlet Blue (MSB) staining was also performed on the occluded vein and analyzed. In addition, both normal-looking and hyper-condensed pyknotic nuclei[20] were manually counted on H&E-stained sections as above. Ultrastructural changes were analyzed on 0.1-µm ultrathin epoxy resin sections stained with uranyl acetate and lead citrate and viewed by TEM (JEM-1400; Jeol, Tokyo, Japan).

Immunohistochemistry

Sections 6 µm thick were cut on a Leica 2040 microtome. Deparaffinized sections underwent antigen retrieval (permeabilization). Sections were treated with 3% hydrogen peroxide and incubated with blocking serum, followed by primary antibody, mouse anti-human CD163, a marker for porcine macrophages[21] (Novus Biologicals, Littleton, CO), and thereafter with relevant secondary antibody and biotinylated goat anti-mouse followed by use of the VECTASTAIN Elite ABC HRP Kit (Vector Laboratories, Burlingame, CA) and ImmPACT AEC Kit (Vector Laboratories) peroxidase substrate solution according to the manufacturer's instructions. After each incubation three 3-minute PBS washes were performed. Primary antibody in control sections was replaced by isotype control, mouse immunoglobulin G or PBS. Slides were mounted with non-fade mounting medium (Hydromount; National Diagnostics, Atlanta, GA). Sections were viewed and photographed using the Nikon Eclipse E800, and semi-quantification of CD163-positive cells was performed using 60× magnification images.

Statistical Analysis

All data was analyzed using SigmaStat 3.5 (Systat Software, San Jose, CA). For cell death and pyknosis, values are expressed as a fraction (percentage) of total number of cells.[22] The percentage of cell loss for each image was computed and the mean percentage obtained for each group (20 images from 20 sections). Data analysis among groups (normal, untreated, and treated) was performed using one-way analysis of variance, the Mann–Whitney *t*-test, and by Tukey's test. For immunocytochemistry, in each image CD163-positive cells were manually counted. Data analysis among groups (normal, untreated, and treated) was performed using Kruskal–Wallis one-way analysis of variance. $P < 0.05$ was considered as statistically significant. Data are expressed as graphs of mean ± standard error of mean (SEM).

Results

Branch Retinal Vein Occlusion

Immediately after laser treatment of the pig eyes, engorgement of the distal vein and scattered intraretinal hemorrhages were seen in all eyes, indicating an occlusion had been successfully created. The laser burn was clearly distinguishable as a white patch on macroscopic examination of the enucleated eyecups in all of the eyes in which a vein occlusion was induced. LM revealed a thrombus with a central fibrin plug, leucocytes, and coagulated blood cells (Fig. 2).

TUNEL Staining

TUNEL staining revealed apoptotic cells in the GCL and the INL in both treated and untreated BRVO retinas but very few in the normal retina (Fig. 3). The mean ± SEM percentage of TUNEL-positive cells in the GCL in the normal retinas was 5% ± 1.93%. At 2 days, in the untreated BRVO retinas, it was 33% ± 5.02%; in the TA-treated BRVO retinas, 43% ± 6.19%; and in the bevacizumab-treated BRVO retinas, 59% ± 6.32%. At 6 days, in the untreated BRVO retinas it was 1% ± 0.79%; in the TA-treated BRVO retinas, 9% ± 2.30%; and in the bevacizumab-treated BRVO retinas, 11% ± 1.18%. At 10 days, in the untreated BRVO retinas, it was 1% ± 0.39%; in the TA-treated BRVO retinas, 10% ± 2.76%; and in the bevacizumab-treated BRVO retinas, 63% ± 5.51%. At 20 days in the untreated BRVO retinas, it was 3% ± 1.88%; in the TA-treated BRVO retinas, 34% ± 5.74%;

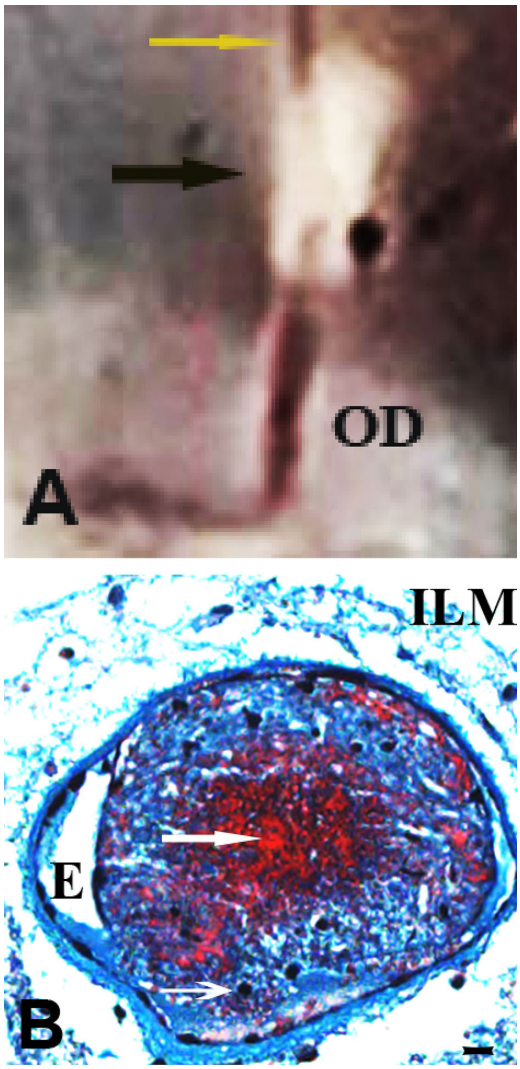

Figure 2. Photothrombotic branch retinal vein occlusion. (**A**) Macroscopic view of the eyecup of a drug-treated BRVO retina at 2 days after surgery displaying the laser burn (*black arrow*) adjacent to the optic disc (OD) that is clearly distinguishable, with the blood flow in the retinal vein (*yellow arrow*) attenuated in the area of the laser burn. (**B**) Light micrograph of retina at 2 days after surgery in which BRVO was attempted showing the vein lined by endothelial cells (E) and the lumen of the vein occupied almost completely by a thrombus packed with clumped red blood cells, leucocytes (*thin arrow*), and fibrin-stained red (*thick arrow*). *Scale bar*: 8 µm.

and in the bevacizumab-treated BRVO retinas, 61% ± 4.69%.

Quantification of the percentage of TUNEL-positive cells in the GCL showed significantly higher levels of apoptosis in the bevacizumab-treated compared to TA-treated retinas at 2, 10, and 20 days after BRVO ($P < 0.05$). The percentage of TUNEL-positive cells was significantly higher in the bevacizumab-treated group at all time points and in the

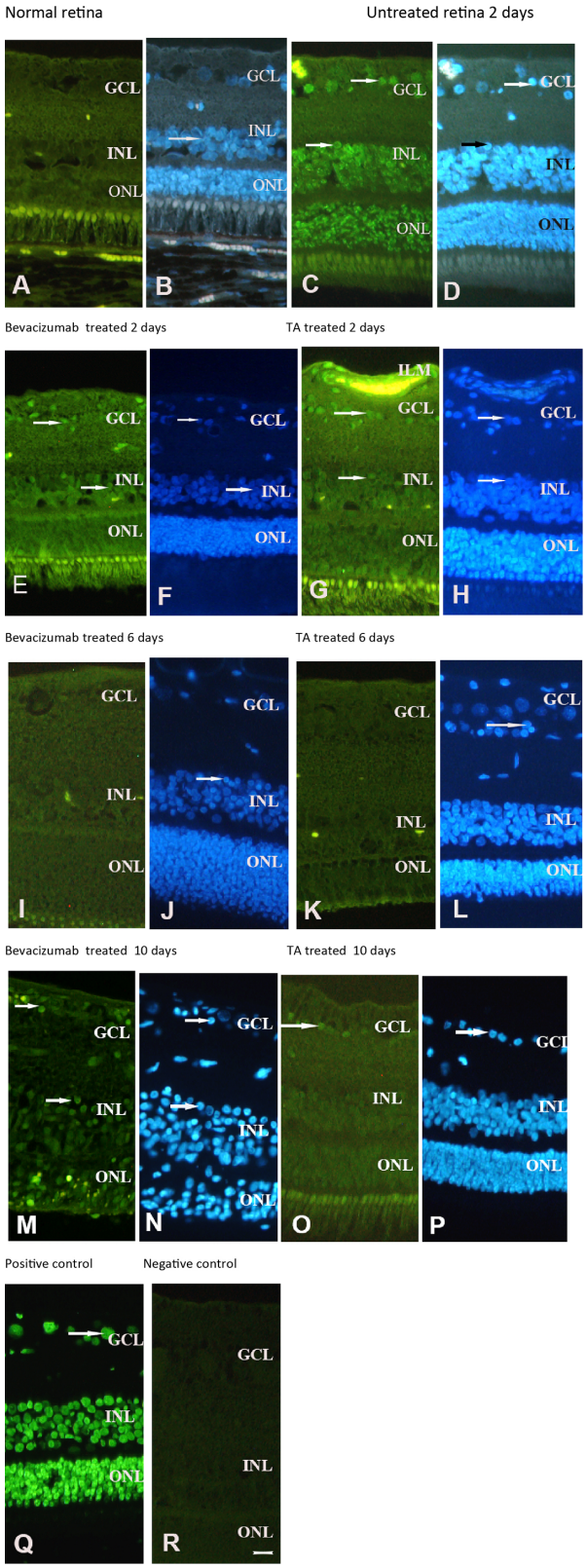

Figure 3. TUNEL labeling. TUNEL-stained cell green fluorescence (excitation, 450–490 nm; *arrows*) and Hoechst-stained cell blue fluorescence (excitation, 330–380 nm; arrows) are seen in the GCL, INL, and outer nuclear layer (ONL). (**A**, **B**) Normal retina; (**C**, **D**) untreated retina; (**E**, **F**) bevacizumab-treated retina; (**G**, **H**) TA-treated retina; (**I**, **J**) bevacizumab-treated retina; (**K**–**Q**) positive control; (**R**) negative control. *Scale bar*: 17 µm.

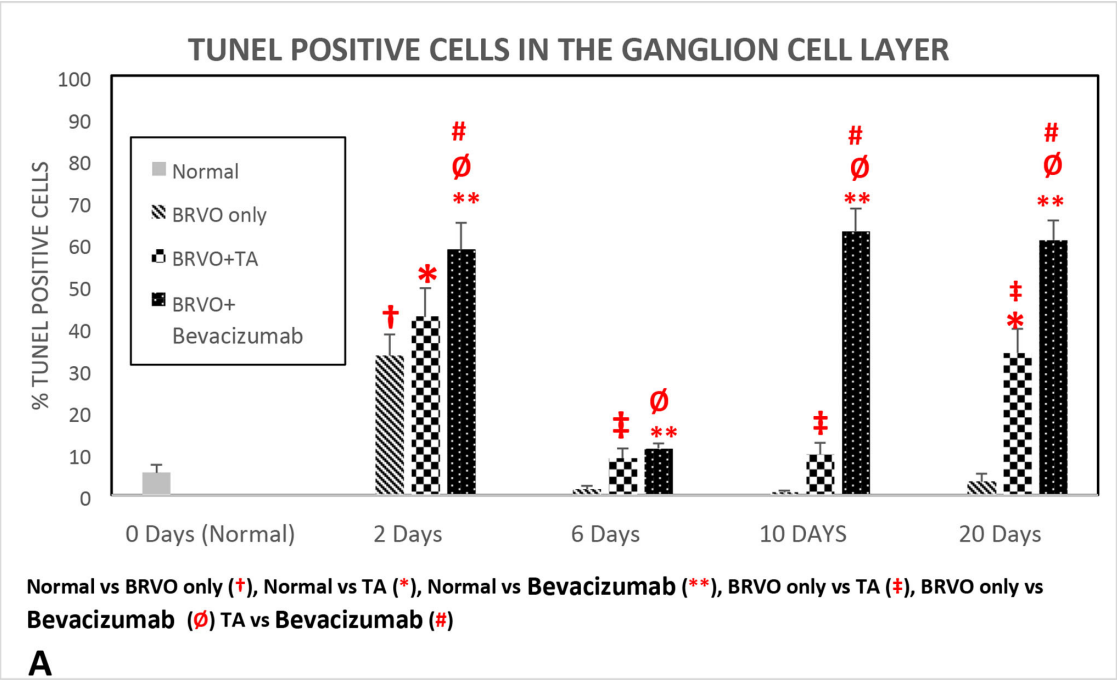

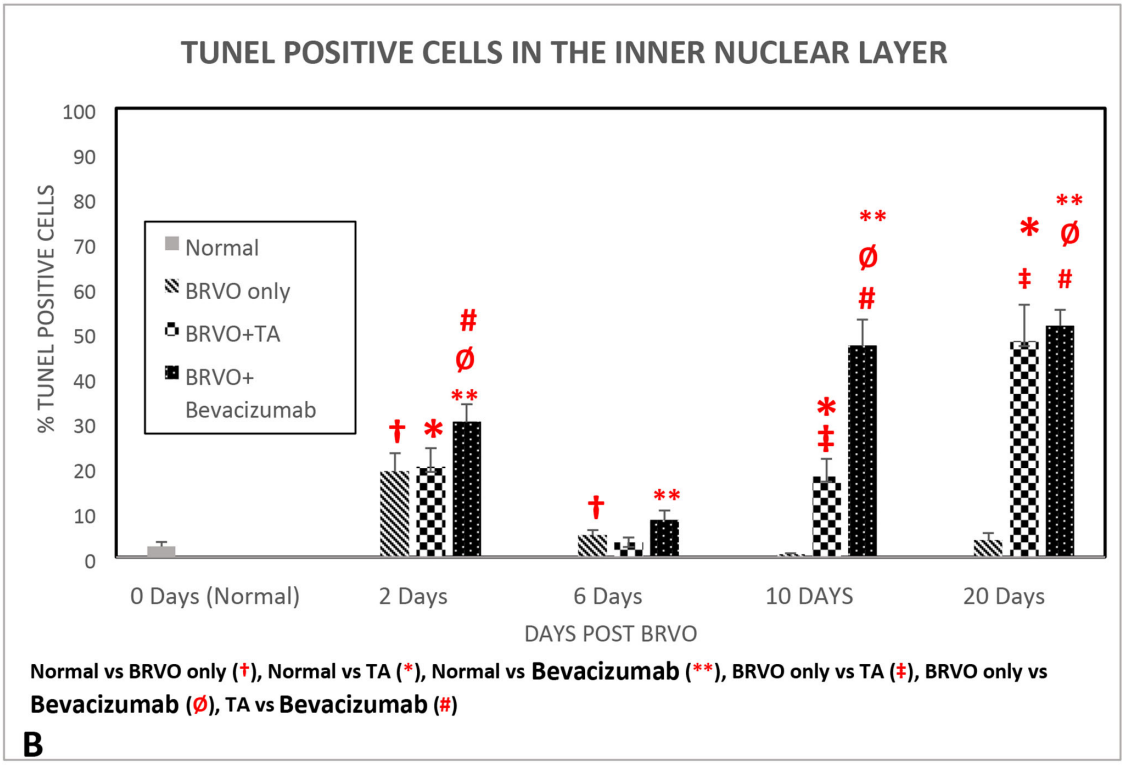

Figure 4. Graph showing mean ± SEM percentage of dying TUNEL-positive cells. Higher significance of TUNEL-positive cell counts is indicated as follows: †normal versus untreated BRVO only, *normal versus TA-treated BRVO, **normal versus bevacizumab-treated BRVO, ‡untreated versus TA-treated BRVO, Øuntreated versus bevacizumab-treated BRVO, and #TA versus bevacizumab-treated BRVO. (**A**) In the ganglion cell layer; (**B**) in the inner nuclear layer. Each bar of the treated eyes represents the mean data from 20 sections taken from five eyes from five pigs; each bar of the untreated eyes and normal eyes represents 20 sections taken from five eyes from three pigs.

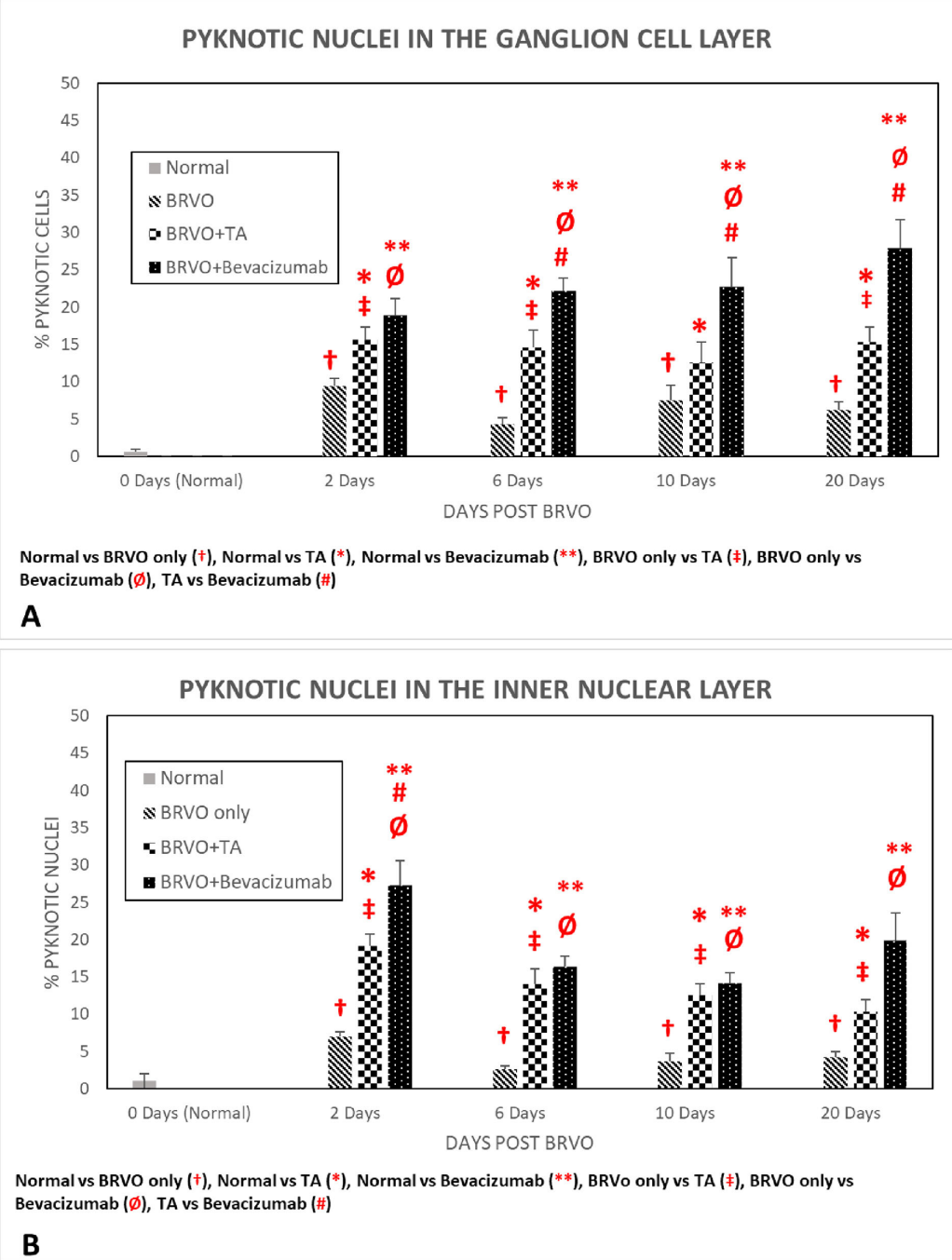

Figure 5. Graph showing mean ± SEM percentage of pyknotic nuclei. Higher significance of pyknotic cell counts is indicated by the following symbols: †normal versus untreated BRVO only, *normal versus TA-treated BRVO, **normal versus bevacizumab-treated BRVO, ‡untreated versus TA-treated BRVO, Øuntreated versus bevacizumab-treated BRVO, and #TA versus bevacizumab-treated BRVO (**A**) In the ganglion cell layer; (**B**) in the inner nuclear layer. Each bar of the treated eyes represents the mean data from 20 sections taken from five eyes from five pigs; each bar of the untreated eyes and normal eyes represents 20 sections taken from five eyes from three pigs.

TA-treated BRVO group at 2 and 20 days compared to the normal retinas ($P < 0.05$). They were also significantly higher in the bevacizumab-treated group at all time points and in the TA-treated BRVO group at 6, 10, and 20 days ($P < 0.05$) compared to untreated BRVO retinas. Significantly higher percentages of apoptotic cells were seen in the untreated BRVO retinas compared to normal retinas at 2 days after

BRVO ($P < 0.05$). Apoptotic cell numbers were not statistically significant in the other pairwise comparisons (TA-treated vs. bevacizumab-treated at 6 days; TA-treated versus normal at 6 and 10 days; TA-treated vs. untreated at 2 days after BRVO; untreated vs. normal at 6, 10, and 20 days after BRVO) ($P > 0.05$) (Fig. 4A).

The mean ± SEM percentage of TUNEL-positive cells in the INL in the normal retina was 2% ± 1.0%. At 2 days in the untreated BRVO retinas, it was 19% ± 4.09%; in the TA-treated BRVO retinas, 20% ± 4.29%; and in the bevacizumab-treated BRVO retinas, 30% ± 4.01%. At 6 days, in the untreated BRVO retinas it was 5% ± 1.13%; in the TA-treated BRVO retinas, 3% ± 1.12%; and in the bevacizumab-treated BRVO retinas, 8% ± 2.17%. At 10 days, in the untreated BRVO retinas, it was 1% ± 0.31%; in the TA-treated BRVO retinas, 18% ± 4.05%; and in the bevacizumab-treated BRVO retinas, 47% ± 5.94%. At 20 days, in the untreated BRVO retinas it was 4% ± 1.64%; in the TA-treated BRVO retinas, 48% ± 8.19%; and in the bevacizumab-treated BRVO retinas, 52% ± 3.56%.

In the INL, quantification of the percentage of apoptotic cells was significantly higher in the bevacizumab-treated retinas compared to the TA-treated retinas at 2, 10, and 20 days after BRVO ($P < 0.05$). The percentages were significantly higher in the bevacizumab-treated retinas at all time points and in the TA-treated BRVO retinas at 2, 10, and 20 days after occlusion compared to normal retinas ($P < 0.05$).

The percentage of apoptotic cells were also significantly higher in bevacizumab-treated retinas at 2, 10, and 20 days and in the TA-treated retinas at 10 and 20 days after occlusion compared to untreated BRVO retinas ($P < 0.05$). Significantly higher percentages of apoptotic cells were seen in the untreated BRVO retinas compared to normal retinas at 2 and 6 days after occlusion. Apoptotic cell numbers were not significant in the other pairwise comparisons (TA-treated vs. bevacizumab-treated at 6 days after occlusion; TA-treated vs. normal at 6 days after occlusion; bevacizumab-treated vs. untreated at 6 days after occlusion; TA-treated vs. untreated at 2 and 6 days after occlusion; normal vs. untreated at 10 and 20 days after occlusion; $P > 0.05$) (Fig. 4B).

Pyknosis

Pyknotic cells displayed condensed dark nuclei in the GCL and INL on H&E sections viewed by LM. The mean ± SEM percentage of pyknotic cells in the GCL in the normal retina was 1% ± 0.39%. At 2 days, in the untreated BRVO, it was 9% ± 1.02%; in the TA-treated BRVO, 16% ± 1.69%; and in the bevacizumab-treated BRVO, 19% ± 2.20%. At 6 days, in the untreated BRVO, it was 4% ± 0.88; in the TA-treated BRVO, 15% ± 2.35%; and in the bevacizumab-treated BRVO, 22% ± 1.64%. At 10 days, in the untreated BRVO, it was 7% ± 1.20%; in TA-treated BRVO, 13% ± 2.74%; and in the bevacizumab-treated BRVO, 23% ± 3.91%. At 20 days, in the untreated BRVO, it was 6% ± 1.02%; in the TA-treated BRVO, 15% ± 2.01%; and in the bevacizumab-treated BRVO, 28% ± 3.76%.

In the GCL, the percentage of pyknotic cells was significantly higher in the bevacizumab-treated retinas compared to the TA-treated retinas at 6, 10, and 20 days after BRVO ($P < 0.05$). Pyknosis was significantly higher in the bevacizumab- and TA-treated BRVOs at all time points compared to the normal retina ($P < 0.05$). They were also significantly higher in the bevacizumab-treated BRVOs compared to the untreated BRVOs at all time points, whereas in the TA-treated BRVOs apoptotic cells were significant at 2, 6, and 20 days ($P < 0.05$), with no significance at 10 days after BRVO ($P > 0.05$). A significantly higher percentage of pyknotic cells were seen in the untreated BRVO retinas compared to normal retinas at all time points ($P < 0.05$). There was no significant difference in the other pairwise comparisons (bevacizumab-treated vs. TA-treated at 2 days after BRVO; TA-treated vs. untreated at 10 days after BRVO) (Fig. 5A).

The mean ± SEM percentage of pyknotic cells in the INL in the normal retina was 1% ± 0.26%. At 2 days, in the untreated BRVO, it was 7% ± 0.62%; in the TA-treated BRVO, 19% ± 1.62%; and in the bevacizumab-treated BRVO, 27% ± 3.31%. At 6 days, in the untreated BRVO, it was 3% ± 0.44%; in the TA-treated BRVO, 14% ± 1.97%; and in the bevacizumab-treated BRVO, 16% ± 1.35%. At 10 days, in the untreated BRVO, it was 4% ± 1.06%; in TA-treated BRVO, 13% ± 1.53%; and in the bevacizumab-treated BRVO, 14% ± 1.35%. At 20 days, in the untreated BRVO, it was 4% ± 0.75%; in the TA-treated BRVO, 10% ± 1.53%; and in the bevacizumab-treated BRVO, 20% ± 3.66%.

The percentage of pyknotic cells in the INL was significantly higher in the bevacizumab-treated retinas compared to the TA-treated retinas at 2 days after BRVO ($P < 0.05$), whereas there was no significant difference between bevacizumab-treated and TA-treated retinas at 6, 10, and 20 days after BRVO ($P > 0.05$). They percentages were also significantly higher in the bevacizumab- and TA-treated BRVOs at all time points compared to normal and untreated BRVOs ($P < 0.05$) (Fig. 5B).

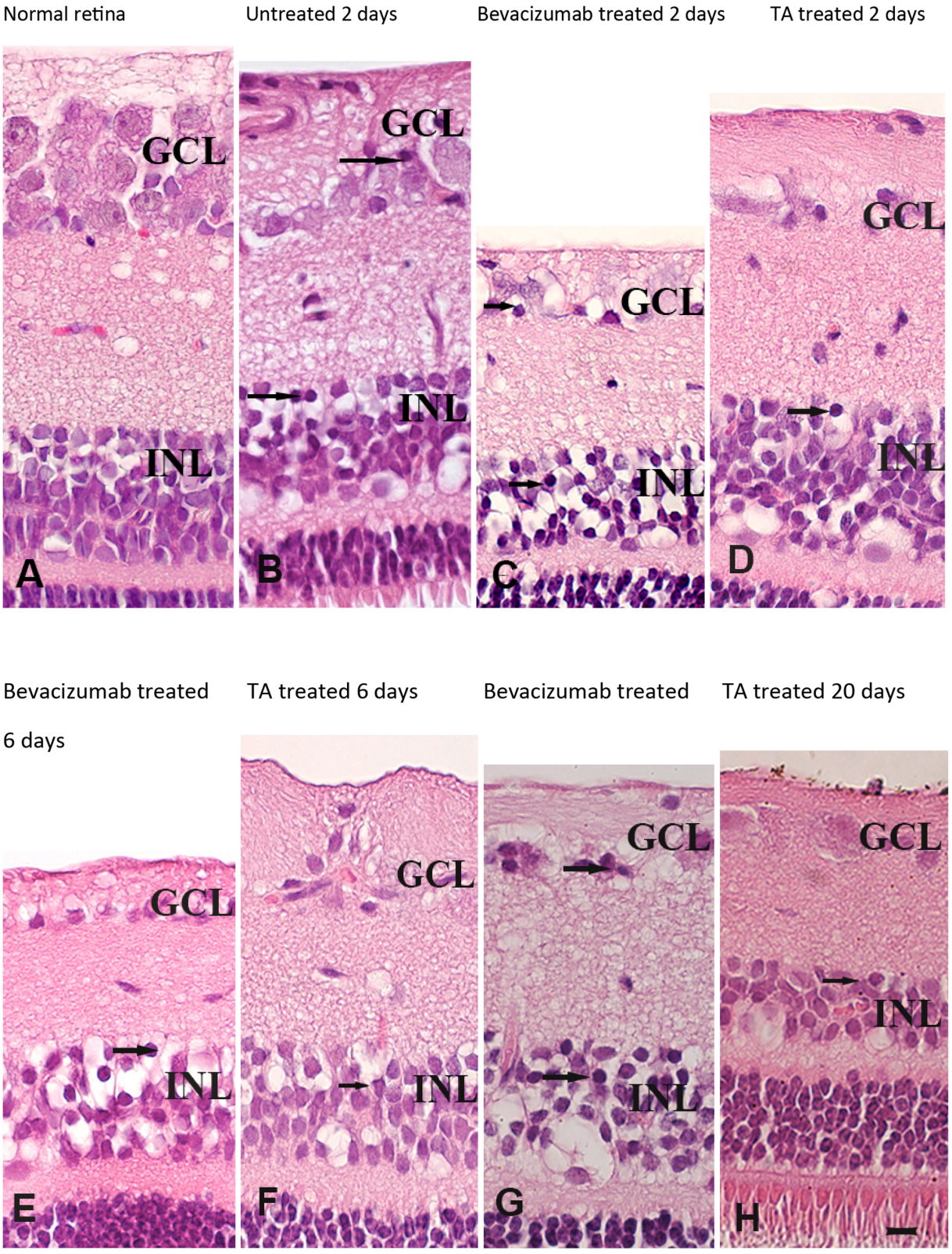

Figure 6. Histology–light microscopy. Light micrographs of (**A**) normal retina, (**B**) untreated retina, (**C**) bevacizumab-treated retina, (**D**) TA-treated retina, (**E**) bevacizumab-treated retina, (**F**) TA-treated retina, (**G**) bevacizumab-treated retina, and (**H**) TA-treated retina. Pyknotic cells (*arrow*) in the GCL and in the INL in the untreated and treated retina are seen. *Scale bar*: 10 µm.

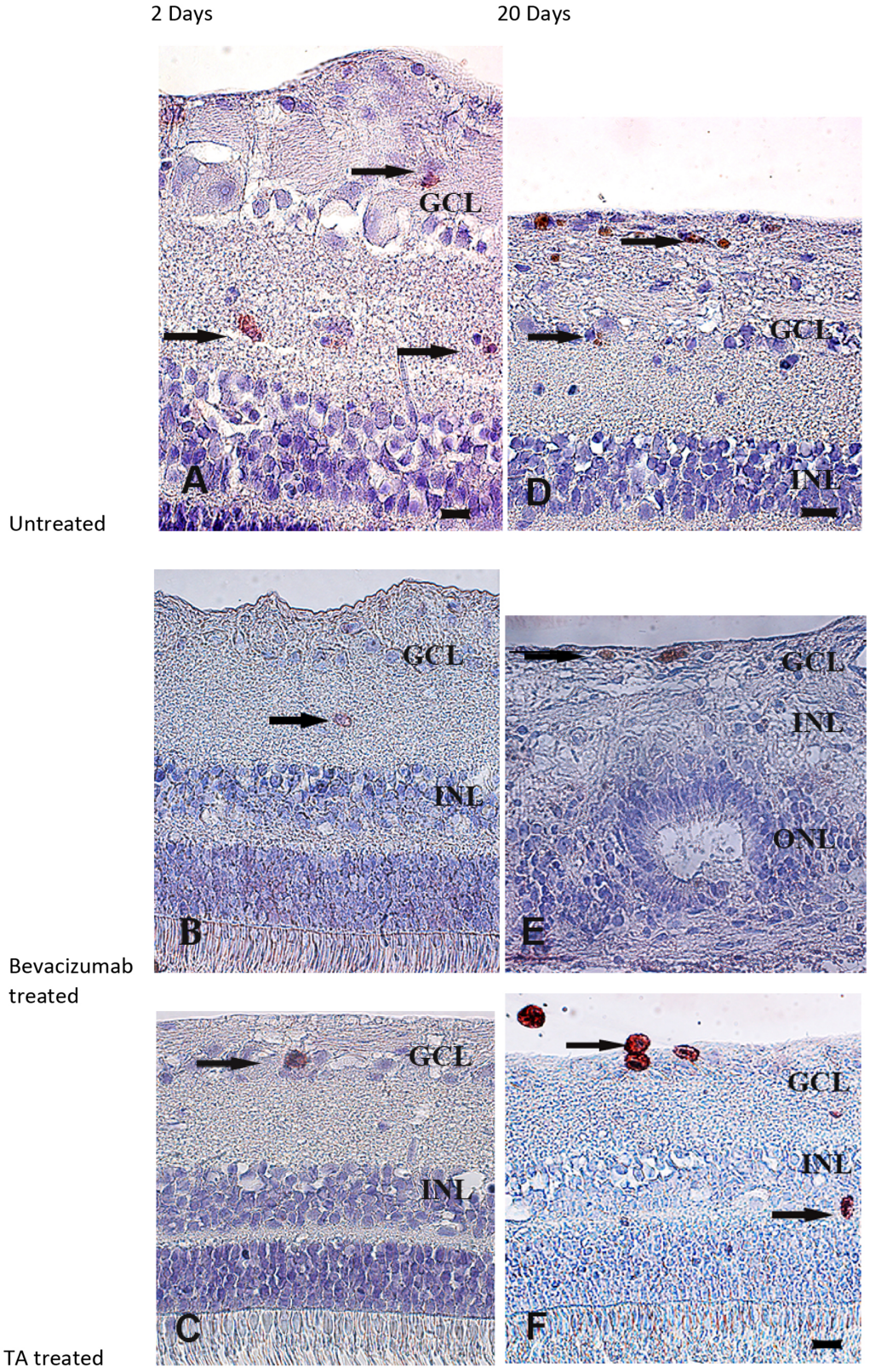

Figure 7. Immunohistochemistry of CD163 (macrophages) counterstained with Hematoxylin in untreated BRVO and TA-treated and bevacizumab-treated retinas at 2 and 20 days after occlusion. Immunolocalization of CD163 at 2 days after occlusion: (**A**) untreated, (**B**) bevacizumab-treated, and (**C**) TA-treated BRVO. At 20 days after occlusion: (**D**) untreated, (**E**) bevacizumab-treated, and (**F**) TA-treated BRVO. Staining of macrophages (*arrow*) is seen predominantly in the GCL, IPL in the INL, inner limiting membrane, and vitreous cavity. Disruption of the outer nuclear layer (ONL) with displacement of nuclei and a vacuole containing debris of rod outer segments can be seen in the TA-treated BRVO at 20 days after occlusion (F). *Scale bar*: 25 µm.

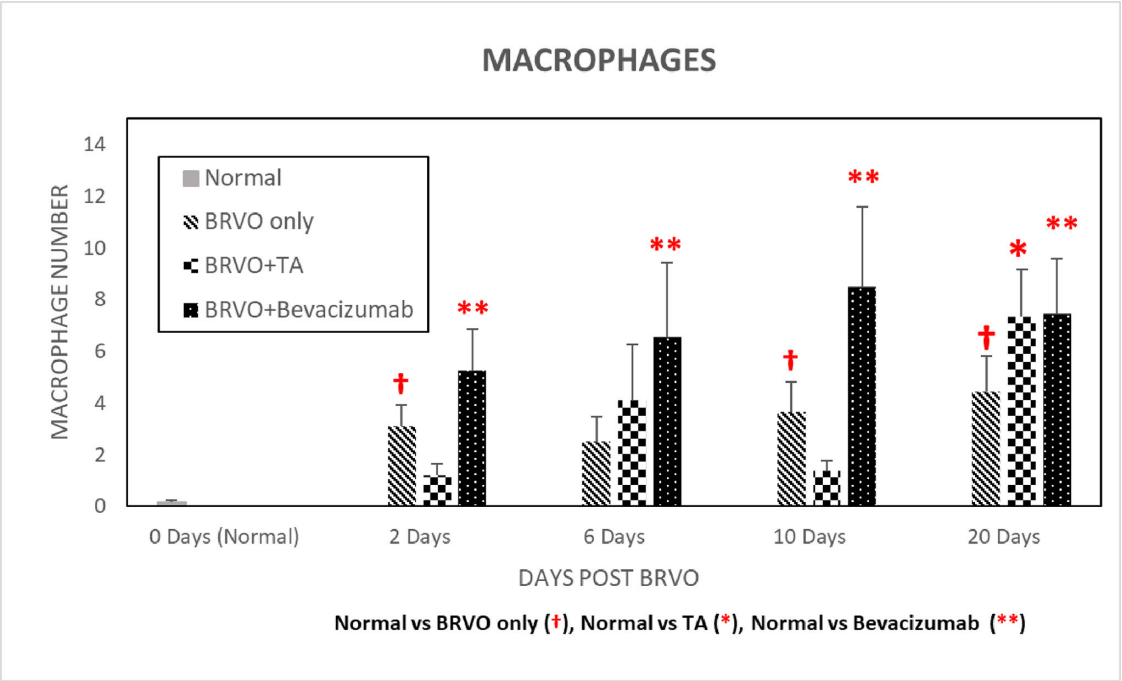

Figure 8. Graph showing mean ± SEM of macrophages in untreated BRVO, TA-treated, and bevacizumab-treated retinas. Higher significance of macrophage counts is indicated by the following symbols: †normal versus untreated BRVO; *normal versus TA-treated BRVO; and **normal versus bevacizumab-treated BRVO. Each bar of the treated eyes represents the mean data from 20 sections taken from five eyes from five pigs; each bar of the untreated eyes and normal eyes represents 20 sections taken from five eyes from three pigs.

Morphology

Basic histology of the normal retinas showed healthy, well-organized layers of cells, whereas the eyes with untreated and treated BRVO revealed degenerative changes in the cells of the IRLs at all time points. Vacant spaces and pyknotic nuclei were seen in the GCL and the INL. There was some variability in the thickness of the retina in both the untreated and treated eyes (Fig. 6).

Immunohistochemistry

CD163 immunoreactivity in macrophages was clearly distinguishable in the vitreous and the inner retina and was otherwise rare in the outer retina in untreated and treated BRVO retina at all time points (Fig. 7). There was scarce immunoreactivity in the normal retina. Immunostaining of the control retinas, in which the primary antibody was omitted or replaced with an isotype control antibody, demonstrated an absence of specific staining. The mean ± SEM number of macrophages of 20 sections across five pigs was 0 ± 0.09 in the normal retina. At 2 days, in the untreated BRVO, it was 3 ± 0.83; in the TA-treated BRVO, 1 ± 0.44; and in the bevacizumab-treated BRVO, 5 ± 1.62. At 6 days, in the untreated BRVO, it was 3 ± 0.96; in the TA-treated BRVO, 4 ± 2.15; and in the bevacizumab-treated BRVO, 7 ± 2.89. At 10 days, in the untreated BRVO, it was 4 ± 1.15; in the TA-treated BRVO 1 ± 0.37; and in the bevacizumab-treated BRVO, 9 ± 3.09. At 20 days, in the untreated BRVO, it was 4 ± 1.39; in the TA-treated BRVO, 7 ± 1.81; and in the bevacizumab-treated BRVO, 7 ± 2.13.

Statistical analysis showed a significantly higher number of macrophages in the untreated BRVO retinas at 2, 10, and 20 days after occlusion; in bevacizumab-treated BRVO at all time points (2, 6, 10 and 20 days); and in the TA-treated BRVO at 20 days after occlusion compared to normal retina ($P < 0.05$). There was no significant difference in the other comparisons: normal versus untreated BRVO at 6 days after occlusion; normal versus TA-treated BRVO at 2, 6, and 10 days after occlusion; untreated BRVO versus bevacizumab- and TA-treated BRVO at all time points (2, 6, 10, and 20 days); and TA-treated versus bevacizumab-treated BRVO at all time points ($P > 0.05$) (Fig. 8).

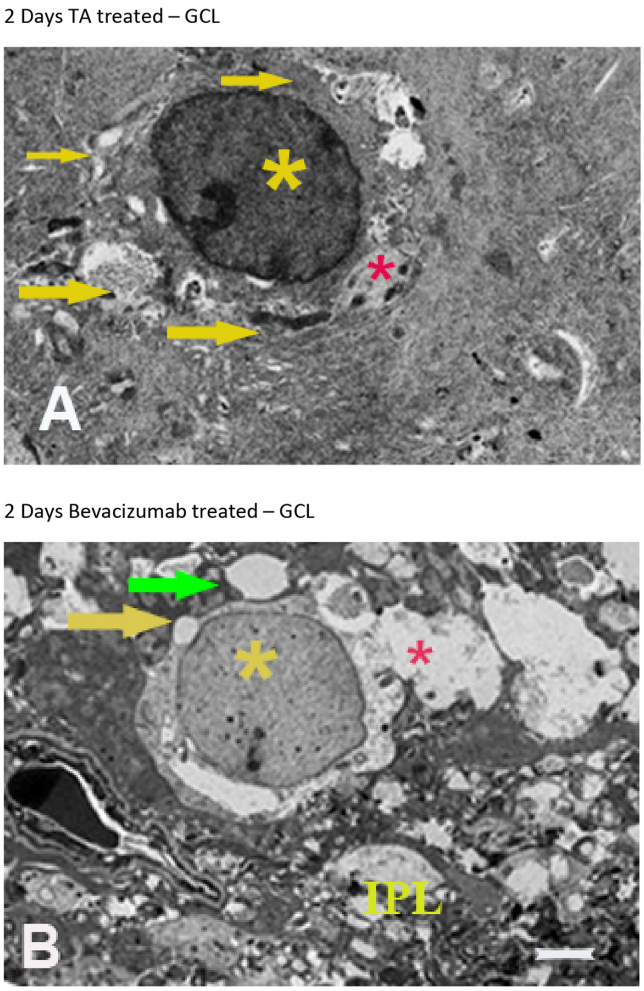

Figure 9. Ultrastructural changes indicated by TEM of the TA- and bevacizumab-treated retinas showing apoptosis in the NFL and in the GCL at 2 days after occlusion. (**A**) In the TA-treated eye, in the NFL close to the inner limiting membrane, an apoptotic cell (*yellow**) with periphralizing. Of chromatin and with several buds from the plasma membrane containing organelles (*arrow*) and chromatin-like fragments (*red**). (**B**) In the bevacizumab-treated eye, at the border between the IPL and GCL, an apoptotic cell (*) with budding of the plasma membrane (*yellow arrow*) and extruded apoptotic bodies with (*red**) and without (*green arrow*) organelles, progressing toward cell death. *Scale bar*: 1.5 µm.

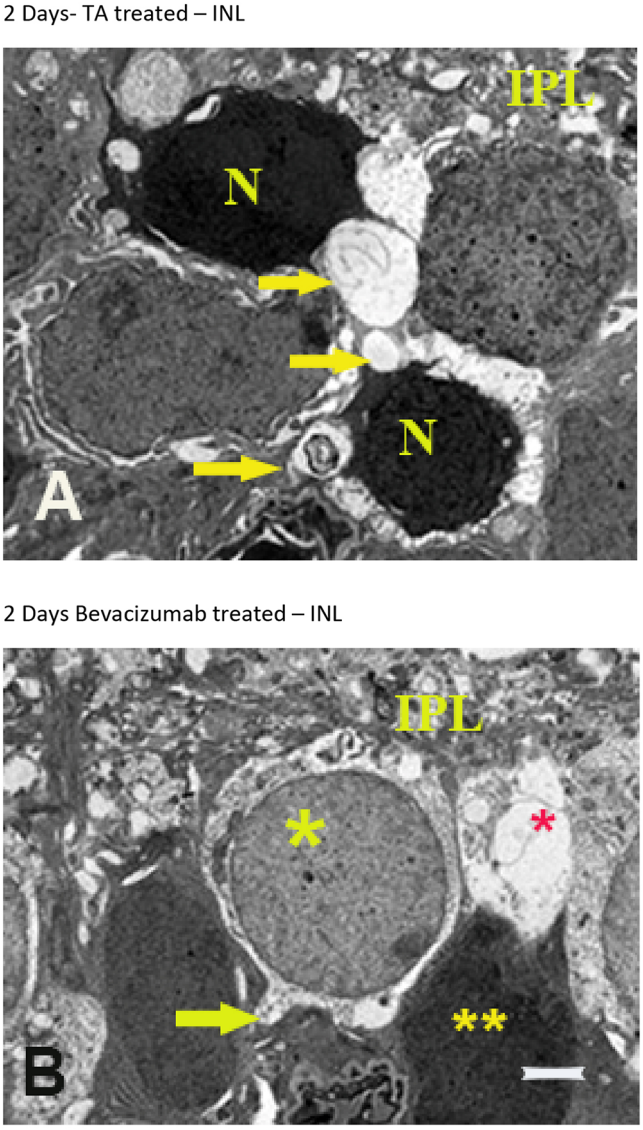

Figure 10. Ultrastructural changes indicated by TEM of the TA- and bevacizumab-treated retinas showing apoptosis in the INL at 2 days after occlusion. (**A**) In the TA-treated eye, at the border between the IPL and INL, two apoptotic cells with electron-dense hyperchromatic nuclei (N) and several buds (*yellow arrow*) containing fragments of organelles, in an advanced stage. (**B**) In the bevacizumab-treated eye, at the border between the IPL and INL, an apoptotic cell (*yellow**) with budding (*yellow arrow*) and next to a Müller cell (**) with a large bud containing fragments of organelles (*red**) in advanced stages. *Scale bar*: 1.5 µm.

TEM in untreated and treated BRVO confirmed and extended the LM findings. Cells in various stages of apoptosis were observed, including those that at the early stages had undergone alterations in their nuclei such as condensation and marginalization of chromatin typical of apoptotic cells. More advanced stages were seen in cells with bleb formation (budding) in the cytosol at the cell surface, resulting in irregular cell membrane and cells with extruded membrane-bound apoptotic bodies, some with and some without fragments of organelles and chromatin-like material. End stages were also seen with macrophages and neutrophils phagocytosing dead cells. In addition, cells that had undergone necrosis were observed (Figs. 9–12).

20 Days TA treated – GCL

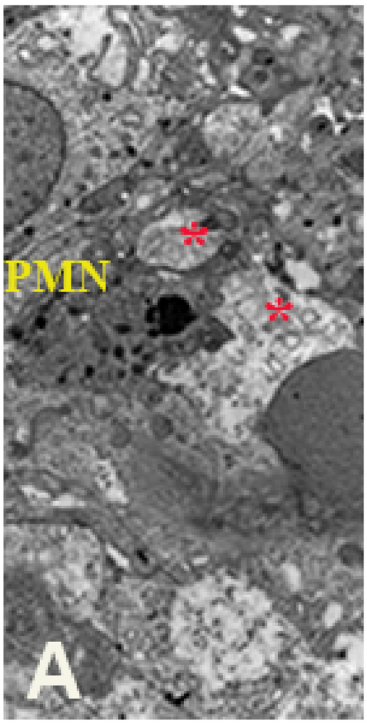

20 Days Bevacizumab treated – GCL

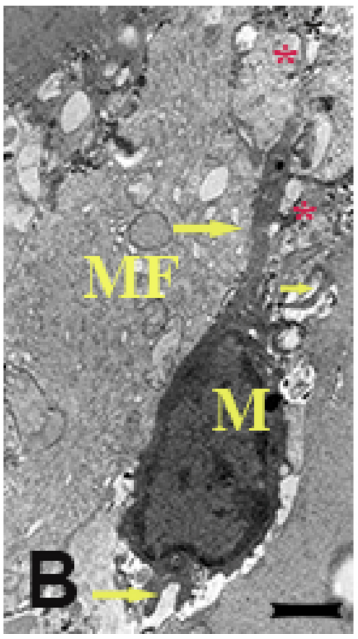

Figure 11. Ultrastructural changes indicated by TEM of the TA- and bevacizumab-treated retinas showing apoptosis in the GCL at 20 days after occlusion. (**A**) In the TA-treated eye, in the GCL, close to the inner limiting membrane, polymorphonucleocyte (PMN) phagocytosing debris (*red**) of a necrotic cell. (**B**) In the bevacizumab-treated eye next to a Müller fiber (MF), a macrophage (M) with several pseudopodia (*yellow arrow*) engulfing most likely apoptotic bodies (*red**) at the end stage of apoptosis. *Scale bar*: 1.5 µm.

20 Days- TA treated – INL

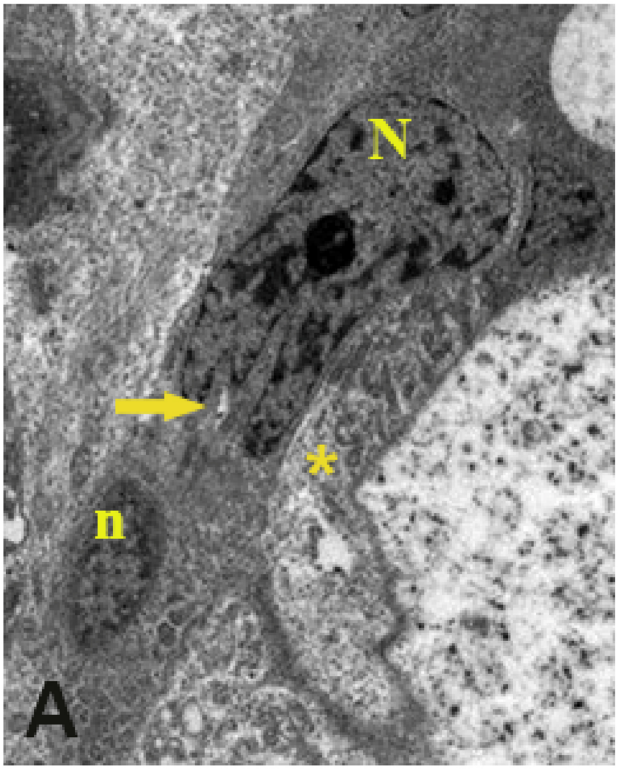

20 Days Bevacizumab treated – INL

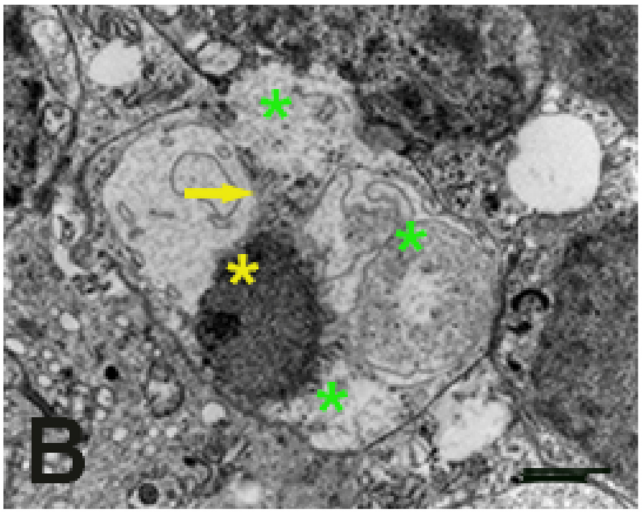

Figure 12. Ultrastructural changes indicated by TEM of the TA- and bevacizumab-treated retinas showing apoptosis in the INL at 20 days after occlusion.(**A**) In the TA-treated eye, in the INL, close to the outer plexiform layer (OPL), an apoptotic cell with a nucleus (N) with a disrupted nuclear membrane (*arrow*) and a fragmented section of membrane-bound nucleus (n) next to a degenerating cell (*yellow**) with shrunken nucleus. (**B**) In the bevacizumab-treated eye, in the INL, close to the OPL, an apoptotic cell with shrinking of the nucleus (*yellow**), chromatin condensing and periphralizing with fragments in the cytoplasm (*yellow arrow*), and aggregation and compartmentalization of organelles (*green**) in the cytoplasm at the early stage of apoptosis. *Scale bar*: 1.5 µm.

Discussion

The inner retinal changes seen in this study could potentially be induced both by the ischemia secondary to the BRVO or the consequences of bevacizumab and triamcinolone acetonide. The results from this study may provide information on the most appropriate timing of intravitreal therapies. Apoptosis is a highly complex process involving an energy-dependent cascade of molecular events. Mitochondrial damage and activation of a group of enzymes belonging to the cysteine protease family of caspases have been proposed as the main changes leading to apoptosis in ischemia.[12,23] During the early stages of apoptosis, cells undergo pyknosis, with condensation and margination of chromatin and shrinking of the cell. There is a potential for the rescue of these cells at this stage.[24] Further chromatin condensation and fragmentation, karyorrhexis, plasma membrane blebbing, and formation of buds consisting of cytoplasm and organelles with or without nuclear fragments occur, and subsequently changes in the cell membrane occur that enable recognition and phagocytosis by macrophages.[23,25] Apoptotic cells can be engulfed by phagocytes even before the formation of apoptotic bodies.[23] Apoptosis of retinal ganglion cells can be very slow and variable in the early stages of retinal disease such as diabetic retinopathy in humans, where they are in a pre-apoptotic state undergoing pyknosis (nuclei with hypercondensed DNA) not detected by TUNEL staining (dead cells with fragmented DNA).[14] This has also been demonstrated in previous studies of RVO in mini pigs[12] and in pre-diabetic retinopathy post mortem eyes where apoptosis and retinal damage occur early.[26]

It has been shown that apoptosis can be reversed in certain circumstances by removing the apoptotic inducers, and in addition it has been shown that apoptosis can be reversed at a later stage in some cells despite caspase activation.[24] The reversal of apoptotic processes by DNA repair has been demonstrated in experimental models of diabetic retinopathy in mice where leukostasis, cell death, and vascular permeability were prevented by the inhibition of tumor necrosis factor alpha (TNFα).[27] There appears to be a window of opportunity in the early stages of apoptosis prior to the "point of no return" when it can be reversed, and therefore the potential for rescuing cells destined to complete the journey to apoptosis in RVOs may exist. As the success in raising public and referrer awareness with macular degeneration has led to earlier presentations of patients with both this condition and other causes of unilateral visual loss including BRVOs, this has enabled patients to be treated much earlier in the acute stage of this vascular condition. In both the current and a previous study,[15] pyknosis did not cease instantaneously and continued up to 20 days after occlusion. This would potentially provide a reasonable period of time for possible neuroprotective agents to be effectively administered to modulate the associated pathways and rescue the less damaged vulnerable cells that are at an early and potentially reversible phase of apoptosis. This could also be a period of increased vulnerability for these cells to any potential agent that reduces native intraretinal cytokines that offer some degree of neuroprotection such as VEGF.

To investigate the effects of bevacizumab and TA in BRVO, the pig model was chosen due to its histological retinal similarity to that of the human. Currently, pig models are used extensively in the evolution of human health research due to their similarities in anatomy, physiology, and genetics. In the eye, similarities to the human in anatomy, vasculature, marker distribution, and histogenesis progression increase the probability of recapitulating human eye diseases more closely compared to other animal models.[28–30] Among non-primate models, pigs have been suggested as the best model for BRVO, and such models have been successfully created in studies in the past, including several of our own.[15,31–33] This very acute type of obstruction that we have been able to achieve in the pig model is rare in humans, where the obstruction to venous outflow occurs at an arteriovenous crossing and is more commonly progressive over variable periods of time. It is, however, useful as an investigative model, as the exact time point of the obstruction is known and the sequence of molecular changes within the retina can be plotted over a known period of time. In a BRVO, there is a variable degree of impaired venous flow resulting in retinal ischemia and hypoxia.[34,35] Under hypoxic conditions, hypoxia inducible factor 1 stimulates VEGF synthesis and changes in the expression of a cascade of multiple inflammatory cytokines, proteins, and factors. VEGF is the main cytokine implicated in these diseases, and some of the highest vitreous concentrations in retinal disorders are seen in RVOs.[35]

VEGF is present in normal adult eyes in the absence of retinal injury. VEGF is a neurotrophic factor present in the central nervous system, retina, and retinal nerve fiber layer. VEGF is essential during the development, growth, and maintenance of retinal vascularization and is a physiological factor expressed in the normal adult retina. It is a critical neuroprotectant during the response to ischemic injury.[16] It is secreted by several cells in the retina, including retinal pigment epithelial cells, neurons, glial cells, endothelial cells, ganglion cells, Müller cells, and smooth muscle cells.[36] It is essential for the preservation of neurons. Consequently,

it was speculated that, if intraretinal VEGF is reduced in the very early phases of the vascular occlusion, as seen in our previous study[15] and in other studies,[37–39] then anti-VEGF therapy in this acute phase may potentially further exacerbate neuronal cell death by apoptosis. This study therefore was undertaken to ascertain if neuroprotection is impaired by early treatment with bevacizumab therapy and compare this to the steroid TA, which possesses a broader spectrum of properties both anti-inflammatory and neuroprotective, despite also inhibiting VEGF, although to a lesser extent than a VEGF antibody such as bevacizumab.[40]

In this study, apoptosis and pyknosis were observed in both the treated and untreated retinas with BRVOs. Incomplete execution of the apoptotic process in cells can lead to necrosis due to the reduction of caspases and adenosine 5′-triphosphate.[41,42] TUNEL may not discriminate between necrotic and apoptotic cells; however, TEM is considered to be the unequivocal gold standard and most accurate method for the detection of apoptotic cells.[42] In this study, TEM confirmed TUNEL staining and revealed apoptosis in various stages, including the engulfment of apoptotic cells by phagocytes. Similar results were observed by Donati et al.,[12] who demonstrated that neuronal cell death related to apoptosis was the prominent feature in the absence of any significant necrosis in experimental BRVO in minipigs. In this study, the BRVO appears to induce an early wave of apoptosis in the GCL and INL at 2 days, which is exacerbated by bevacizumab treatment and to a lesser extent by TA. This decreases by 6 days, presumably because most of the sensitive and less resilient cells have succumbed to the initial injury and the more robust cells have survived, resulting in fewer apoptotic cells. This is followed by a second wave seen at the 10- and 20-day time points in the bevacizumab- and TA-treated eyes but not in the eyes with BRVO only. Pyknosis is slightly different, with both treated groups having higher levels of pyknotic nuclei from 2 to 20 days than the untreated BRVO retinas. Bevacizumab-treated retinas tended to have higher levels than TA-treated retinas from 6 to 20 days, predominantly in the GCL. Pyknosis in the untreated BRVO retinas peaked at 2 days and fell to lower levels from 6 to 20 days. TEM was performed to confirm the intracellular changes seen by LM in respect to both the stages of apoptosis and pyknotic nuclear changes rather than quantifying cellular numbers. Some variation in retinal thickness was seen in some of the untreated and treated eyes, which may reflect in part individual variations. For those receiving BRVO injuries, the resulting variable levels of apoptosis are likely to have resulted in some variation in thinning of the retina, depending on the differing rates in treated and untreated retinas. Previously, significant decreases in thickness in the nerve fiber layer (NFL) and inner plexiform layer (IPL) in BRVO patients has been reported.[43–45] In general apoptosis and pyknosis were increased in the bevacizumab-treated retinas compared to the TA-treated retinas, and our hypothesis is that this increase is due to the blockage of VEGF which reduces neuroprotection. Greater degrees of change were seen in eyes treated with bevacizumab, which is a direct VEGF antagonist. Although TA can also indirectly reduce VEGF, it is to a lesser extent,[40] reflecting lesser degrees of apoptosis and pyknosis compared to bevacizumab in this study.

Macrophages may also be associated with the increase in apoptosis. It has been demonstrated that macrophages can contribute to cell death.[46] Deletion of macrophages results in the survival of endothelial cells.[47,48] Elimination of macrophages in the anterior chamber of rat eye resulted in the survival of endothelial cells that normally would have undergone apoptosis.[46]

There was an infiltration of a considerable number of macrophages in both the untreated and treated eyes, with higher levels of infiltration in the bevacizumab-treated retinas, as seen by LM and TEM. Bevacizumab may possibly induce some inflammatory changes due to retention of the Fc portion in this full-length humanized antibody.[49] Unexpected results were also seen with the use of bevacizumab in human choroidal neovascularization, where higher levels of macrophages were seen in the treated group compared to controls.[50] Commercial TA formulations may also contribute to the recruitment of macrophages in animal models. Dispersions of exposed TA crystals within the vitreous are phagocytic targets for macrophages.[51] However, this study found that the TA-treated retinas showed little overall difference when compared to untreated BRVOs.

Anti-VEGF drugs have become the mainstay treatment for RVOs and other retinal vascular diseases and have resulted in significant improvements in visual outcomes compared to the natural history of these conditions. Visual outcomes can be variable and most do require ongoing treatment.[52,53] There is also some concern about potential adverse effects of anti-VEGF therapy. It has been demonstrated that repeated VEGF blockade has been associated with both GCL and NFL loss,[50–53] although the exact mechanism is uncertain. Although this effect may be minimal in those receiving these treatments for macular degeneration, the loss of the neuroprotective effect of VEGF might be greater for those with more extensive retinal vascular disease. In patients with RVO receiving VEGF inhibitors, optical coherence tomography studies have revealed thinning of the NFL and inner

retina, despite resolution of the ME.[54–56] We have previously shown that the responses in the acute phase of BRVO include inflammation as seen by the upregulation of inflammatory cytokines and breakdown of osmohomeostasis by the dislocation of the Ki 4.1 water channel. Although bevacizumab targets VEGF, it has no effect on the host of inflammatory cytokines that are upregulated and promote inflammation in these diseases. Inflammation may also play a potential role in the pathogenesis of BRVO,[57] and targeting this may be important in the acute phase to reduce neurodegeneration.

To the best of our knowledge, this work investigating neurodegeneration in inner retinal tissue in the pig model in acute BRVO has not been performed previously. Most of the previous studies have used aqueous and vitreous samples in both human and other animal models and do not reflect the exact sequence of intraretinal events, especially in the acute phases of this condition. Investigation in the acute phase as early as 2 days in BRVO patients at the molecular level has not been performed before, and these findings may be unknown in the human. This photothrombotic pig model produces an occlusion that is acute and relatively more severe than the slow and progressive occlusion and retinal changes seen in most patients with a BRVO. A steroid, in this study in the form of TA, showed a better neuroprotective outcome compared to bevacizumab in the acute phase of BRVO in this pig model. VEGF does not appear to be upregulated immediately, and it is possible that early treatment with antagonists to this cytokine, which in itself has neuroprotective capabilities, before it is fully upregulated may be counterproductive, but there are vulnerable, damaged neural elements that may potentially be able to be rescued. Anti-VEGF therapy may be effective at a later stage in the evolution of BRVO when ME and intraretinal leakage occur. Timing of anti-VEGF therapy may be important in the early phase of the progression of the disease to limit further damage to retinal neural elements. As a first line of treatment in an acute presentation of BRVO, potentially a single dose of a steroid preparation such as TA or the dexamethasone implant[52] may be more protective and effective in the treatment of acute BRVO before commencing the current standard of care of using anti-VEGF agents. The data presented in this study are limited to a very acute and relatively severe experimental BRVO. Although this study does indicate that retinal neural cells in the acute phase of a BRVO are vulnerable to VEGF blockade, the relevance of this to the clinical treatment of patients with this condition is uncertain. Most clinical presentations occur outside this time period and often with variable levels of severity and ischemia, so any extrapolation from this study to clinical management of BRVO is limited. Further investigation into the development of potentially better and more effective neuroprotective agents is required.

Acknowledgments

Supported by a grant from the National Health and Medical Research Council of Australia (APP1173403 to D-YY) and by a WA Near Miss Award (MRFF1142962 to FKC).

Disclosure: **I.L. McAllister**, None; **S. Vijayasekaran**, None; **R. Bhikoo**, None; **F.K. Chen**, None; **D. Zhang**, None; **E. Kanagalingam**, None; **S. McLenachan**, None; **D.-Y. Yu**, None

References

1. Wong TY, Scott IU. Clinical practice. Retinal-vein occlusion. *N Engl J Med*. 2010;363:2135–2144.
2. Rogers S, McIntosh RL, Cheung N, et al. The prevalence of retinal vein occlusion: pooled data from population studies from the United States, Europe, Asia, and Australia. *Ophthalmology*. 2010;117:313–319.e1.
3. Mitchell P, Smith W, Chang A. Prevalence and associations of retinal vein occlusion in Australia. The Blue Mountains Eye Study. *Arch Ophthalmol*. 1996;114:1243–1247.
4. Klein R, Klein BE, Moss SE, Meuer SM. The epidemiology of retinal vein occlusion: the Beaver Dam Eye Study. *Trans Am Ophthalmol Soc*. 2000;98:133–141.
5. Rogers SL, McIntosh RL, Lim L, et al. Natural history of branch retinal vein occlusion: an evidence-based systematic review. *Ophthalmology*. 2010;117:1094–1101.e5.
6. The Branch Vein Occlusion Study Group. Argon laser photocoagulation for macular edema in branch vein occlusion. *Am J Ophthalmol*. 1984;98:271–282.
7. Heath Jeffery RC, Mukhtar SA, McAllister IL, Morgan WH, Mackey DA, Chen FK. Inherited retinal diseases are the most common cause of blindness in the working-age population in Australia. *Ophthalmic Genet*. 2021;42:431–439.
8. Awdeh RM, Elsing SH, Deramo VA, Stinnett S, Lee PP, Fekrat S. Vision-related quality of life in persons with unilateral branch retinal vein occlusion using the 25-item National Eye Institute

Visual Function Questionnaire. *Br J Ophthalmol*. 2010;94:319–323.
9. Ip MS, Scott IU, VanVeldhuisen PC, et al. A randomized trial comparing the efficacy and safety of intravitreal triamcinolone with observation to treat vision loss associated with macular edema secondary to central retinal vein occlusion: the Standard Care vs Corticosteroid for Retinal Vein Occlusion (SCORE) study report 5. *Arch Ophthalmol*. 2009;127:1101–1114.
10. Brown DM, Campochiaro PA, Bhisitkul RB, et al. Sustained benefits from ranibizumab for macular edema following branch retinal vein occlusion: 12-month outcomes of a phase III study. *Ophthalmology*. 2011;118:1594–1602.
11. Campochiaro PA, Clark WL, Boyer DS, et al. Intravitreal aflibercept for macular edema following branch retinal vein occlusion: the 24-week results of the VIBRANT study. *Ophthalmology*. 2015;122:538–544.
12. Donati G, Kapetanios A, Dubois-Dauphin M, Pournaras CJ. Caspase-related apoptosis in chronic ischaemic microangiopathy following experimental vein occlusion in mini-pigs. *Acta Ophthalmol*. 2008;86:302–306.
13. Joo CK, Choi JS, Ko HW, et al. Necrosis and apoptosis after retinal ischemia: involvement of NMDA-mediated excitotoxicity and p53. *Invest Ophthalmol Vis Sci*. 1999;40:713–720.
14. Abu-El-Asrar AM, Dralands L, Missotten L, Al-Jadaan IA, Geboes K. Expression of apoptosis markers in the retinas of human subjects with diabetes. *Invest Ophthalmol Vis Sci*. 2004;45:2760–2766.
15. McAllister IL, Vijayasekaran S, Zhang D, McLenachan S, Chen FK, Yu DY. Neuronal degeneration and associated alterations in cytokine and protein in an experimental branch retinal venous occlusion model. *Exp Eye Res*. 2018;174:133–146.
16. Nishijima K, Ng YS, Zhong L, et al. Vascular endothelial growth factor-A is a survival factor for retinal neurons and a critical neuroprotectant during the adaptive response to ischemic injury. *Am J Pathol*. 2007;171:53–67.
17. Alon T, Hemo I, Itin A, Pe'er J, Stone J, Keshet E. Vascular endothelial growth factor acts as a survival factor for newly formed retinal vessels and has implications for retinopathy of prematurity. *Nat Med*. 1995;1:1024–1028.
18. Gaballa SA, Kompella UB, Elgarhy O, et al. Corticosteroids in ophthalmology: drug delivery innovations, pharmacology, clinical applications, and future perspectives. *Drug Deliv Transl Res*. 2021;11:866–893.
19. Bancroft JD, Stevens A. *Theory and Practice of Histological Techniques*, 6th ed. London: Churchill Livingstone; 2008.
20. Crowley LC, Marfell BJ, Waterhouse NJ. Detection of DNA fragmentation in apoptotic cells by TUNEL. *Cold Spring Harb Protoc*. 2016;2016:pdbprot087221.
21. Greising SM, Rivera JC, Goldman SM, Watts A, Aguilar CA, Corona BT. Unwavering pathobiology of volumetric muscle loss injury. *Sci Rep*. 2017;7:13179.
22. Crowley LC, Marfell BJ, Scott AP, et al. Dead cert: measuring cell death. *Cold Spring Harb Protoc*. 2016;2016:pdbtop070318.
23. Wong RS. Apoptosis in cancer: from pathogenesis to treatment. *J Exp Clin Cancer Res*. 2011;30:87.
24. Tang HL, Tang HM, Mak KH, et al. Cell survival, DNA damage, and oncogenic transformation after a transient and reversible apoptotic response. *Mol Biol Cell*. 2012;23:2240–2252.
25. Elmore S. Apoptosis: a review of programmed cell death. *Toxicol Pathol*. 2007;35:495–516.
26. Barber AJ, Lieth E, Khin SA, Antonetti DA, Buchanan AG, Gardner TW. Neural apoptosis in the retina during experimental and human diabetes. Early onset and effect of insulin. *J Clin Invest*. 1998;102:783–791.
27. Huang H, Gandhi JK, Zhong X, et al. TNFα is required for late BRB breakdown in diabetic retinopathy, and its inhibition prevents leukostasis and protects vessels and neurons from apoptosis. *Invest Ophthalmol Vis Sci*. 2011;52:1336–1344.
28. Groenen MA, Archibald AL, Uenishi H, et al. Analyses of pig genomes provide insight into porcine demography and evolution. *Nature*. 2012;491:393–398.
29. Douglas WR. Of pigs and men and research: a review of applications and analogies of the pig, sus scrofa, in human medical research. *Space Life Sci*. 1972;3:226–234.
30. Guduric-Fuchs J, Ringland LJ, Gu P, Dellett M, Archer DB, Cogliati T. Immunohistochemical study of pig retinal development. *Mol Vis*. 2009;15:1915–1928.
31. McAllister IL, Vijayasekaran S, Khong CH, Yu DY. Investigation of the safety of tenecteplase to the outer retina. *Clin Exp Ophthalmol*. 2006;34:787–793.
32. McAllister IL, Vijayasekaran S, Yu DY. Intravitreal tenecteplase (metalyse) for acute management of retinal vein occlusions. *Invest Ophthalmol Vis Sci*. 2013;54:4910–4918.
33. McAllister IL, Vijayasekaran S, Chen SD, Yu DY. Effect of triamcinolone acetonide on vascular

endothelial growth factor and occludin levels in branch retinal vein occlusion. *Am J Ophthalmol*. 2009;147:838–846, 846.e1–2.
34. Rehak J, Rehak M. Branch retinal vein occlusion: pathogenesis, visual prognosis, and treatment modalities. *Curr Eye Res*. 2008;33:111–131.
35. Aiello LP, Avery RL, Arrigg PG, et al. Vascular endothelial growth factor in ocular fluid of patients with diabetic retinopathy and other retinal disorders. *N Engl J Med*. 1994;331:1480–1487.
36. Famiglietti EV, Stopa EG, McGookin ED, Song P, LeBlanc V, Streeten BW. Immunocytochemical localization of vascular endothelial growth factor in neurons and glial cells of human retina. *Brain Res*. 2003;969:195–204.
37. Rehak M, Drechsler F, Koferl P, et al. Effects of intravitreal triamcinolone acetonide on retinal gene expression in a rat model of central retinal vein occlusion. *Graefes Arch Clin Exp Ophthalmol*. 2011;249:1175–1183.
38. Rehak M, Hollborn M, Iandiev I, et al. Retinal gene expression and Müller cell responses after branch retinal vein occlusion in the rat. *Invest Ophthalmol Vis Sci*. 2009;50:2359–2367.
39. Ebneter A, Agca C, Dysli C, Zinkernagel MS. Investigation of retinal morphology alterations using spectral domain optical coherence tomography in a mouse model of retinal branch and central retinal vein occlusion. *PLoS ONE*. 2015;10:e0119046.
40. Sohn HJ, Han DH, Kim IT, et al. Changes in aqueous concentrations of various cytokines after intravitreal triamcinolone versus bevacizumab for diabetic macular edema. *Am J Ophthalmol*. 2011;152:686–694.
41. Denecker G, Vercammen D, Declercq W, Vandenabeele P. Apoptotic and necrotic cell death induced by death domain receptors. *Cell Mol Life Sci*. 2001;58:356–370.
42. Elmore SA, Dixon D, Hailey JR, et al. Recommendations from the INHAND Apoptosis/Necrosis Working Group. *Toxicol Pathol*. 2016;44:173–188.
43. Kim CS, Shin KS, Lee HJ, Jo YJ, Kim JY. Sectoral retinal nerve fiber layer thinning in branch retinal vein occlusion. *Retina*. 2014;34:525–530.
44. Lim HB, Kim MS, Jo YJ, Kim JY. Prediction of retinal ischemia in branch retinal vein occlusion: spectral-domain optical coherence tomography study. *Invest Ophthalmol Vis Sci*. 2015;56:6622–6629.
45. Ahn J, Hwang DD. Peripapillary retinal nerve fiber layer thickness in patients with unilateral retinal vein occlusion. *Sci Rep*. 2021;11:18115.
46. Diez-Roux G, Lang RA. Macrophages induce apoptosis in normal cells in vivo. *Development*. 1997;124:3633–3638.
47. Diez-Roux G, Argilla M, Makarenkova H, Ko K, Lang RA. Macrophages kill capillary cells in G1 phase of the cell cycle during programmed vascular regression. *Development*. 1999;126:2141–2147.
48. Lang RA. Apoptosis in mammalian eye development: lens morphogenesis, vascular regression and immune privilege. *Cell Death Differ*. 1997;4:12–20.
49. Stewart MW. The expanding role of vascular endothelial growth factor inhibitors in ophthalmology. *Mayo Clin Proc*. 2012;87:77–88.
50. Tatar O, Yoeruek E, Szurman P, et al. Effect of bevacizumab on inflammation and proliferation in human choroidal neovascularization. *Arch Ophthalmol*. 2008;126:782–790.
51. Cannon GJ, Swanson JA. The macrophage capacity for phagocytosis. *J Cell Sci*. 1992;101(pt 4):907–913.
52. Wallsh JO, Gallemore RP. Anti-VEGF-resistant retinal diseases: a review of the latest treatment options. *Cells*. 2021;10:1049.
53. Ach T, Hoeh AE, Schaal KB, Scheuerle AF, Dithmar S. Predictive factors for changes in macular edema in intravitreal bevacizumab therapy of retinal vein occlusion. *Graefes Arch Clin Exp Ophthalmol*. 2010;248:155–159.
54. Lima VC, Yeung L, Castro LC, Landa G, Rosen RB. Correlation between spectral domain optical coherence tomography findings and visual outcomes in central retinal vein occlusion. *Clin Ophthalmol*. 2011;5:299–305.
55. Klein R, Moss SE, Meuer SM, Klein BE. The 15-year cumulative incidence of retinal vein occlusion: the Beaver Dam Eye Study. *Arch Ophthalmol*. 2008;126:513–518.
56. Alshareef RA, Barteselli G, You Q, et al. In vivo evaluation of retinal ganglion cells degeneration in eyes with branch retinal vein occlusion. *Br J Ophthalmol*. 2016;100:1506–1510.
57. Noma H, Yasuda K, Shimura M. Cytokines and the pathogenesis of macular edema in branch retinal vein occlusion. *J Ophthalmol*. 2019;2019:5185128.